Environmental Health Perspectives
Vol. 84, pp. 45-56, 1990

An Overview of Techniques for the Measurement of Calcium Distribution, Calcium Fluxes, and Cytosolic Free Calcium in Mammalian Cells

by André B. Borle*

An array of techniques can be used to study cell calcium metabolism that comprises several calcium compartments and many types of transport systems such as ion channels, ATP-dependent pumps, and antiporters. The measurement of total cell calcium brings little information of value since 60 to 80% of total cell calcium is actually bound to the extracellular glycocalyx. Cell fractionation and differential centrifugation have been used to study intracellular Ca^{2+} compartmentalization, but the methods suffer from the possibility of Ca^{2+} loss or redistribution among cell fractions. Steady-state kinetic analyses of ^{45}Ca uptake or desaturation curves have been used to study the distribution of Ca^{2+} among various kinetic pools in living cells and their rate of Ca^{2+} exchange, but the analyses are constrained by many limitations. Nonsteady-state tracer studies can provide information about rapid changes in calcium influx or efflux in and out of the cell. Zero-time kinetics of ^{45}Ca uptake can detect instantaneous changes in calcium influx, while ^{45}Ca fractional efflux ratio, can detect rapid stimulations or inhibitions of calcium efflux out of cells. Permeabilized cells have been successfully used to gauge the relative role of intracellular organelles in controlling $[Ca^{2+}]i$. The measurement of the cytosolic ionized calcium ($[Ca^{2+}]i$) is undoubtedly the most important and, physiologically, the most relevant method available. The choice of the appropriate calcium indicator, fluorescent, bioluminescent, metallochromic, or Ca^{2+}-sensitive microelectrodes depends on the cell type and the magnitude and time constant of the event under study. Each probe has specific assets and drawbacks. The study of plasma membrane vesicles derived from baso-lateral or apical plasmalemma can also bring important information on the (Ca^{2+}-Mg^{2+}) ATPase-dependent calcium pump and on the kinetics and stoichiometry of the Na^+-Ca^{2+}antiporter. The best strategy to study cell calcium metabolism is to use several different methods that focus on a specific problem from widely different angles.

Introduction

Cell calcium metabolism comprises several intra- and extracellular compartments where calcium exchanges occur through a complex array of transporters including three types of calcium channels, two types of (Ca^{2+}-Mg^{2+})ATPase-dependent calcium pumps, and at least one, or perhaps two types of antiporters (Na^+-Ca^{2+} and Ca^{2+}-H^+ exchangers). One of the most important parameters of cell calcium metabolism is the cytosolic ionized calcium ($[Ca^{2+}]_i$).

At rest, the control of $[Ca^{2+}]_i$ is effected through the interplay of the calcium ATPase pump and the Na^+-Ca^{2+} antiporter at the plasmalemma; calcium influx into mitochondria, driven by the inner membrane potential that is established by the proton pump; calcium efflux from mitochondria through a Na^+-Ca^{2+} exchanger and/or an unidentified mitochondrial efflux pathway; and finally, a calcium ATPase pump in the endoplasmic reticulum (Fig. 1). Whether calcium cycles across the endoplasmic reticulum (ER) membrane at rest is not known.

During excitation or after hormonal stimulation, $[Ca^{2+}]_i$ is regulated by a completely new set of transporters. The following calcium channels of several types open in the plasmalemma: voltage-operated channels (VOC), receptors-operated channels (ROC), and intracellular-messengers-operated channels (IMOC) (Fig. 2). Several subtypes of voltage-operated channels have been described (type L, T, N). At the endoplasmic reticulum membrane, inositol triphosphate or other messengers triggers and efflux of calcium, presumably through an intracellular-messenger-operated calcium channel.

Finally, $[Ca^{2+}]_i$ is modulated or influenced by a wide variety of ions or metabolites and by their specific transporters (Fig. 3). The forward or reverse mode of

*Department of Physiology, University of Pittsburgh School of Medicine, Pittsburgh, PA 15261.

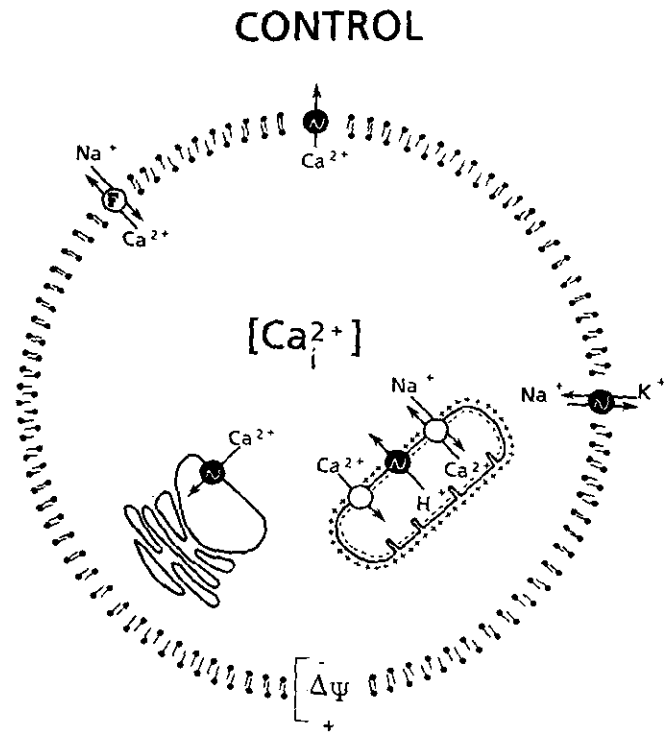

FIGURE 1. Active, ATP-dependent (black circles) and passive (white circles) calcium transport systems contributing to the control of cytosolic free calcium in a resting cell.

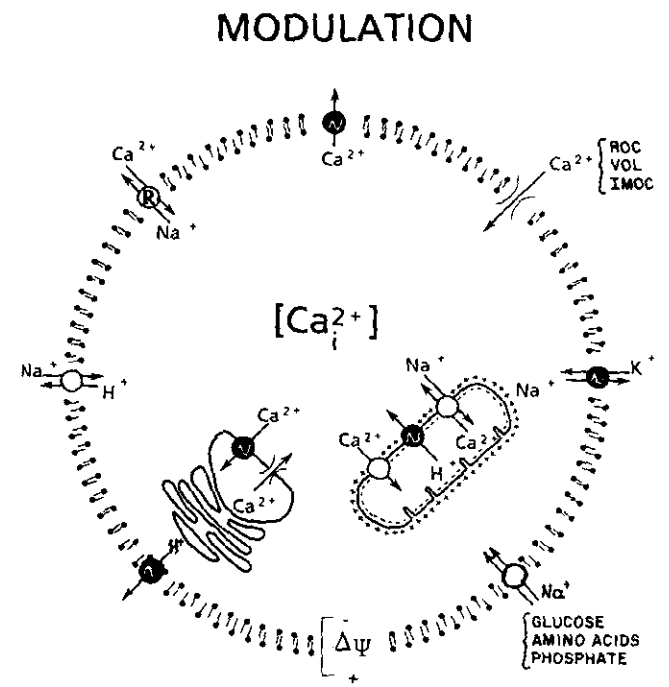

FIGURE 3. Modulators of cytosolic free calcium in a cell at rest: Na^+-K^+ pump, H^+ pump Na^+-H^+antiporters, various Na^+-symporters, and the membrane potential difference $\Delta\psi$ influence $\Delta\mu Na_i^+$, Na^+, the Na^+ electrochemical potential, and the mode of operation of the Na^+-Ca^{2+} antiport that modulates $[Ca^{2+}]_i$.

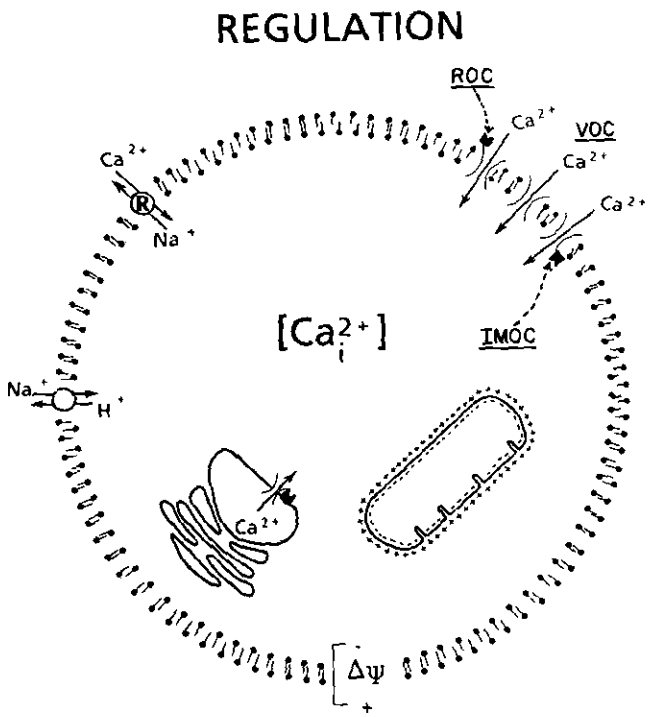

FIGURE 2. Voltage-operated channels (VOC), receptor-operated channels (ROC), intracellular-messenger-operated channels (IMOC) and antiporters reported to respond to specific stimuli regulating cytosolic free calcium in an excited cell.

the Na^+-Ca^{2+}antiporter is thermodynamically determined by the balance between the Na^+ and Ca^{2+} electrochemical potentials. Consequently, the membrane potential, the intracellular and the extracellular Na^+ activity, the (Na-K) ATPase-dependent Na pump, the Na^+-H^+antiporter, intracellular and extracellular pH, the Na^+-glucose and Na^+-amino-acid symporters, and the ATP-dependent proton pumps may all indirectly influence or modulate $[Ca^{2+}]_i$. With such complexity, it is not surprising to find that no single method can ever offer a comprehensive or compelling description of the control, regulation, and modulation of cell calcium metabolism.

Total Cell Calcium

Total cell calcium has been measured by atomic absorption, flame photometry, or by fluorometric titration with calcein as indicator. Table 1, derived from my 1987 review (*1*), shows little difference in cell calcium among various tissues, with a range of 2.1 to 2.7 mmole/kg wet weight. Tumors are an exception with a total cell calcium of 5.5 mmole/kg wet weight. These measurements bring little information since, in most cells, 60 to 80% of the cell calcium is bound to the extracellular cell coat or glycocalyx. Consequently, significant changes in cell calcium metabolism may take place without altering the total cell

Table 1. Total cell calcium of various tissues.[a]

Tissue	Total cell calcium, mmole/kg wet weight
Muscle	2.1
Liver	2.2
Kidney	2.3
Brain	2.7
Miscellaneous	2.4
Tumors	5.5
Naked cells[b]	0.6

[a]From Borle (*1*).
[b]Cells washed with trypsin, EDTA, or EGTA.

calcium. When the extracellularly bound calcium is removed by typsin or by EGTA, the naked cell calcium averages 0.6 mmole/kg wet weight (range 0.4 to 0.9 mmole/kg wet weight).

Cell Fractionation

Cell fractionation and differential ultracentrifugation have often been used to gain further insight into calcium distribution among various cell compartments, in spite of the fact that the methods suffer from possibility of calcium loss or redistribution among the various cell fractions. To minimize such losses or redistribution, EGTA, ruthenium red, and various anesthetics are often added to the homogenizing medium (*2*). The distribution of calcium among compartment varies slightly from tissue to tissue, but the overall percentage shows that most of the cell calcium is sequestered in ER and in mitochondria (Table 2). Since the cell dry weight is approximately 20% of the wet weight and the overall naked cell calcium is 0.6 mmole/kg cell wet weight, mitochondrial calcium is about 1.3 mmole/kg cell dry weight. In liver cells, the ER calcium is about half that of the mitochondria, when expressed on a cell dry weight or cell protein basis. However, since the ER protein is 10% and the mitochondria, 33% of the total cell protein (*3*), the ER calcium concentration is more than twice the mitochondrial calcium per organelle mass. This is in good agreement with recent results obtained with electron microprobes (*4*).

Kinetic Analyses

The kinetic analyses of ^{45}Ca uptake or desaturation curves were developed to gain some insight in the calcium distribution among different cell compartments in a living cell and to estimate the rate of calcium exchange between compartments (*5–7*). It was also an attempt to peel off kinetically the large pool of calcium bound to the glycocalyx without using enzymes or ETGA and to obviate the calcium redistribution that may occur during cell fractionation and ultracentrification. The method has many limitations that are not always recognized.

First, these studies must be performed at steady state. Consequently, short-term, transient, or fast-changing events cannot be studied. Second, the kinetic pools obtained do not necessarily represent well-defined anatomical compartments. They usually reflect a collection of subpools. Indeed, unless compartments all differ materially in their behavior, groups of similar compartments will tend to act together, and the kinetic of the central compartment will be indistinguishable from the kinetics of a system of relatively few compartments (*8*). Identification of the pools is therefore tentative and should be supported by other independent measurements. Third, the number of kinetic components cannot be chosen arbitrarily, but must be determined by a precise formula developed by Jacquez (*9*) (Fig. 4). Fourth, the curves must be analyzed by the weighted, nonlinear least square method (Fig. 5) because graphical analysis is too subjective to be acceptable. Fifth, the exponential constants and coefficients of the multiexponential equation or, if one prefers, the slopes and intercepts of the kinetic components do not represent rate constants or compartments as often assumed. That would imply an improbable, pure parallel system with intracellular organelles in

Table 2. Percent distribution of calcium among various cell fractions isolated by ultracentrifugation.[a]

Cell fraction	Calcium as percent of total homogenate
Nucleus and debris	31.3
Mitochondria	43.0
Microsomes	14.2
Supernatant	9.0

[a]From Borle (*1*).

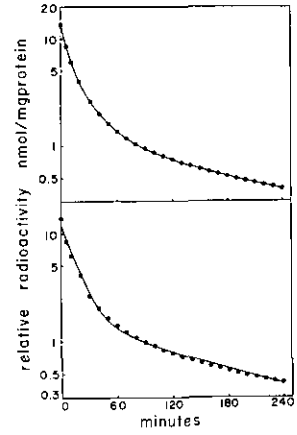

FIGURE 4. Determination of the number of kinetic components by comparing the sum of weighed least squares (*9*). The relative radioactivity of the cells are plotted against time. The points show the data of one typical experiment and the lines show the best fit obtained by nonlinear least square analysis. The same experimental points are shown in both graphs. The upper panel shows the fit obtained for three kinetic phases (sum of weighed least squares = 0.00802); the low panel shows the fit for two kinetic phases (sum of weighed least squares = 0.06211). Reprinted with permission from the *American Journal of Physiology*.

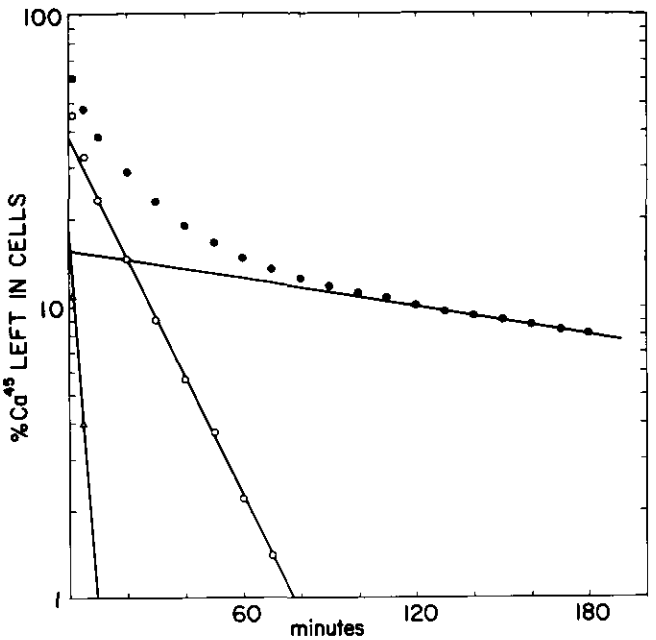

FIGURE 5. Typical ^{45}Ca desaturation curve obtained in isolated kidney cells (LLC-MK_2) in normal Krebs Henseleit buffer containing 1 mM calcium. The three kinetic phases are obtained by nonlinear least square analysis. The slopes and intercepts (or the exponential constants and coefficients) are used to calculate exchangeable pools, exchange rates, and rate constants by a series of equations that varies, depending upon the assumed model system (parallel series or mixed) (*5*).

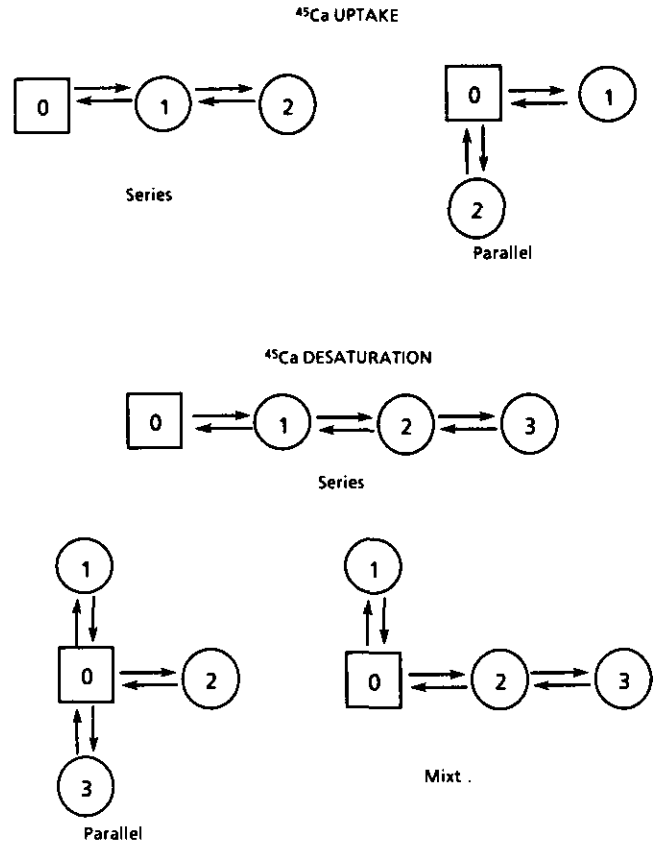

FIGURE 6. Choice of kinetic models that have to be selected for the calculation of the pools, exchange rates, and rate constant from the exponential constants and coefficients obtained from the nonlinear least square analysis of ^{45}Ca uptake curves or ^{45}Ca desaturation curves.

direct contact with the extracellular medium. A symbolic representation of the system must be chosen (series, parallel or mixed) (Fig. 6) based on a believable anatomical description of the model under study. Sixth, steady-state kinetic analysis gives us exchange rates between compartments where influx equals efflux ($\rho ij = J_{ij} = J_{ji}$) so that the results obtained by ^{45}Ca uptake must match those obtained by ^{45}Ca desaturation. One cannot assume that uptake measures calcium influx and desaturation measures calcium efflux.

^{45}Ca uptake experiments can measure the fast and medium kinetic components fairly accurately (Fig. 7), but they cannot detect the third slow component that is less than the usual error of measurement when the curves approach isotopic equilibrium. On the other hand, ^{45}Ca desaturation experiments (Fig. 5) can measure the middle and slow kinetic component with accuracy, while the first fast component usually contains large errors.

Even a careful and formally correct analysis brings a limited amount of information that is not very specific. This information reveals changes in cell calcium distribution and the rate of calcium exchange between different compartments (Table 3), but it cannot detect the primary defect in cell calcium metabolism or the sequence of events leading to the new steady state.

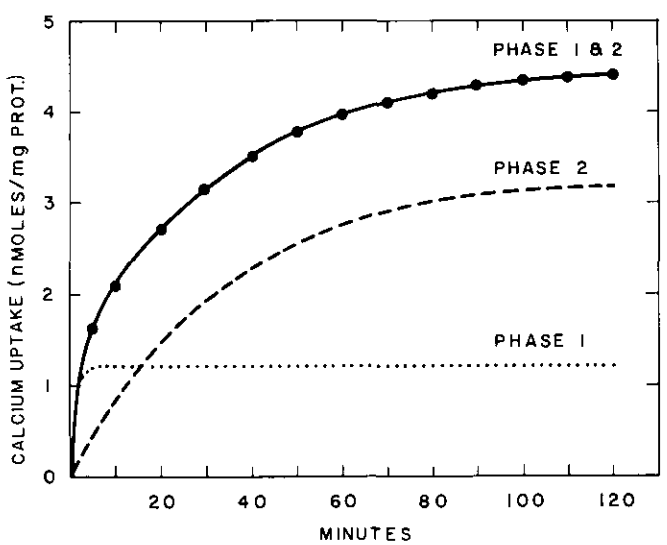

FIGURE 7. Typical ^{45}Ca uptake curve (dots and solid line) separated into its two kinetic components: one first fast phase (dotted line); one second slow phase (dashed line).

Table 3. Changes in cell calcium metabolism expressed as percent of control obtained by kinetic analyses of ^{45}Ca movements in kidney and liver cells.

	Kidney			Liver		
	Acidosis[a]	Alkalosis[a]	HyperPTH[b]	Male/female[c]	Adx[d]	Diabetes[e]
Total Ca	−20	+36	+407	NS	+ 31	NS
^{45}Ca uptake	−38	+13	+133	NS	+ 29	—
^{45}Desaturation						
S_1	NS[f]	+15	+ 73	NS	+ 45	NS
S_2	−41	NS	+233	NS	+ 64	+ 51
S_3	−34	+81	+183	−35	+139	+177
ρ01	NS	+15	NS	−52	+ 57	NS
ρ12	−40	NS	+169	NS	+ 78	NS
ρ23	−34	+75	+220	−46	+119	+220

[a]Studer and Borle (*26*).
[b]Borle and Clark (*27*).
[c]Studer and Borle (*28*).
[d]Studer and Borle (*29*).
[e]Studer (*30*).
NS = not significantly different.

Nonsteady-State Tracer Studies

To study rapid changes in calcium fluxes in and out of cells, we have used nonsteady-state tracer studies. Calcium influx is measured by zero-time kinetics during the first 30 sec of ^{45}Ca uptake, when there is no significant backflux of tracer from cell to medium (Fig. 8). This is done by a rapid separation of the cells from the medium by filtration over a millipore filter and a rapid wash of the extracellularly bound calcium with lanthanum, EGTA, or high calcium wash.

Rapid changes in calcium efflux are measured by the fractional efflux ratio method (*10*). Two groups of cells labeled with ^{45}Ca are desaturated side by side. One group is stimulated and its fractional efflux is compared with that of the unstimulated control (Fig. 9). The fractional efflux ratio gives us the time course of the stimulation and its magnitude; it does not provide the actual rate of calcium efflux.

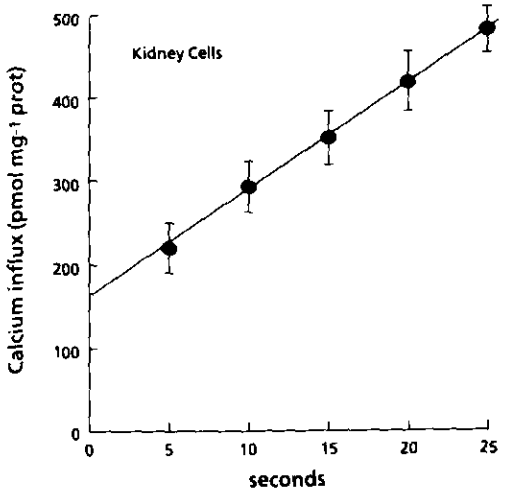

FIGURE 8. Calcium influx measured by ^{45}Ca zero-time kinetics in kidney cell suspension (MDCK). The linearity of the tracer uptake for the first 30 sec is evidence that no significant of detectable tracer backflux is present.

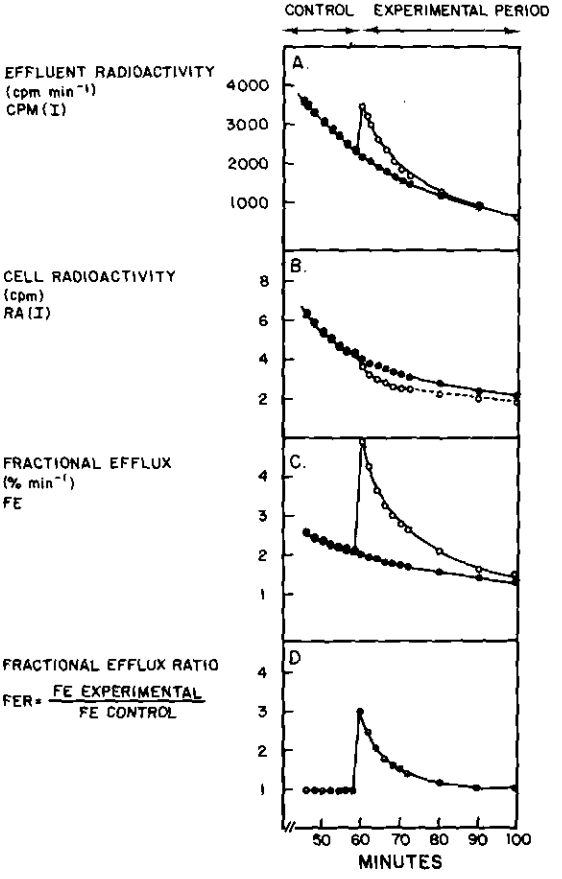

FIGURE 9. Calculation of the calcium fractional efflux ratio. From the radioactivity collected in the effluent (panel A), the cell radioactivity at each time point can be calculated (panel B). Fractional efflux (panel C) is the radioactivity released (panel A) divided by the cell radioactivity (panel B) and the fractional efflux ratio (panel D) is the fractional efflux of an experimental group divided by that of a control group.

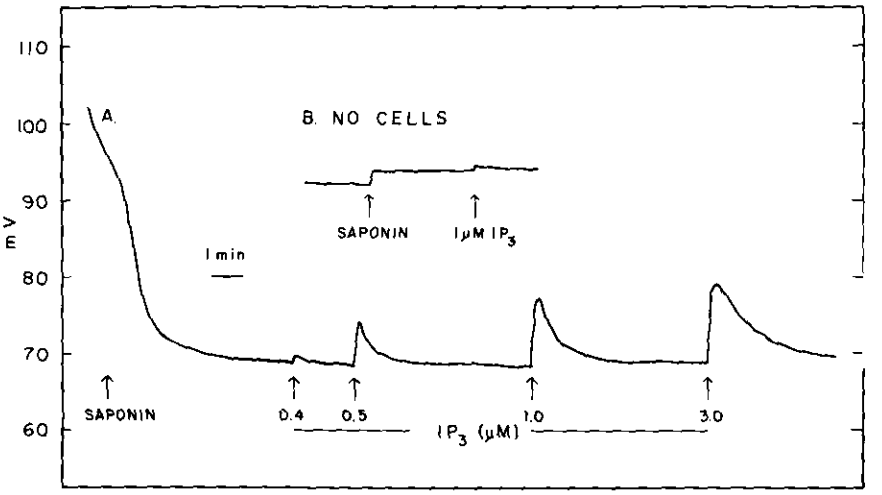

FIGURE 10. Potentiometric recording from a pCa electrode of changes in ionized calcium in the medium of a hepatocyte suspension (*A*) upon the addition of saponin and inositol triphosphate (IP_3). Cells are washed once with Ca-free, Mg-free phosphate-buffered saline containing 1 mM EDTA and then once with a chelexed, Hepes-buffered, saline solution. The cells are resuspended in a cytosollike solution containing ATP and an ATP-regenerating system of enzymes. The ionized calcium in the medium is measured with a calcium-sensitive minielectrode. Additions of saponin (final concentration of 150 μg/mL) and IP_3 are made as indicated. The inset shows the potentiometric recording in the absence of cells upon the additions of saponin and IP_3. From Freudenrich and Borle (*23*); reproduced with permission from the *Journal of Biological Chemistry*.

Permeabilized Cells

To study calcium mobilization from intracellular organelles or the relative importance of the endoplasmic reticulum and the mitochondria in regulating cytosolic free calcium, saponin or digitonin are used to make the cells plasmalemma permeable to ions. The cells are then incubated in a medium assumed to replicate the cytosol composition, i.e., high K, low Ca^{2+}, and an ATP-regenerating system. This method has been used to study the effects of intracellular messengers such as inosotol triphosphate on calcium mobilization from intracellular organelles (Fig. 10). The rise in Ca^{2+} in the medium bathing the permeabilized cells can be measured with arsenazo III, Quin-2, or Ca^{2+}-sensitive microelectrodes. Many investigators use mitochondrial uncouplers, Ca^{2+} ionophores, or drugs such as dantrolene or TMB-8 to induce or block calcium release from one or the other intracellular compartments. The validity of the assumptions regarding the specificity of these agents is not always clear or compelling.

Cytosolic Free Calcium

The most significant breakthrough in the study of cell calcium metabolism in the last 8 years is, undoubtedly, the development of methods to measure cytosolic free calcium $[Ca^{2+}]_i$ in small mammalian cells. The four classes of calcium indicators are shown in Table 4. Their characteristics, relative assets, and drawbacks have already been reviewed (*11–13*).

To this admittedly biased investigator, aequorin is the best calcium indicator; it has a high sensitivity, a high signal-to-noise ratio, a fast response time, and it has no calcium-buffering action or no known side effect on cell function. The past difficulties in incorporating aequorin in small cells have been overcome by the development of several methods applicable to practically all mammalian cells (*14,15*).

Table 4. Intracellular Ca^{2+} probes.

Tetracarboxylate fluorescent indicators
Quin-2
Fura-2
Indo-1
Bis-azo metallochromic indicators
Arsenazo III
Antipyrylazo III
Bioluminescent protein indicators
Aequorin
Obelin
Ca^{2+}-selective microelectrodes
Neutra ligands (ETH 1001)
Organophosphate ligands

On the negative side, the method is not an easy one. It is tedious and time consuming. Great care must be taken to avoid calcium contamination in every solution and all laboratory ware in contact with the photoprotein. The calcium-aequorin reaction is irreversible so that aequorin is constantly being consumed. At the physiological levels of free calcium in the cell, the half-time of aequorin is several weeks (*11*), but above 10^{-5} M Ca^{2+}, aequorin is consumed in minutes.

This characteristic is actually an asset of the method. First, all the aequorin left outside the cell is immediately destroyed by the high extracellular Ca^{2+}. Second, in the unlikely event of an accumulation of aequorin in subcellular organelles, the photoprotein would be inactivated in a matter of minutes by the

high free-calcium concentration presumed to exist in these organelles. Another drawback that is shared with the fluorescent probes is the nonlinearity of the relation between calcium and the light signal. Any inhomogeneity in calcium concentrations within the cells or inhomogeneity in the cell population will distort the average measurement of $[Ca^{2+}]_i$.

The fluorescent probes Quin-2, Fura-2, and Indo-1 are much easier to use and therefore much more popular (*16,17*). They are perhaps best suited for the study of $[Ca^{2+}]_i$ as one element in an otherwise complex system of intracellular signaling. Their best assets are their ease of incorporation as acetoxymethyl esters, the commercial availability of good fluorometers with dual excitation or dual emission, and a fairly straightforward calibration. The main drawbacks are their relatively slow response time, calcium buffering action, side effects on various cell functions, leaking from some cells, and occasional incorporation into subcellular organelles. If one is interested in cellular calcium metabolism per se, and not in cytosolic free calcium as only one of the many steps of a metabolic pathway's sequence of events, it is worth investing the time and effort required by the aequorin methodology.

The metallochromic dyes are the least popular of the four classes of intracellular calcium probes (*18*). They must be introduced into cells by microinjection, they have a low sensitivity and a low signal-to-noise ratio and their calibration in absolute terms is not possible because of the uncertainties regarding the stoichiometry. However, metallochromic dyes do have important qualities: they have the fastest response time of all calcium indicators (less than 10 msec), and the signal is linearly related to the free-calcium activity. Also, they are best suited to detect relative changes at high levels of $[Ca^{2+}]_i$ in very fast events.

The Ca^{2+}-sensitive microelectrodes use the neutral ligand ETH 1001 developed by Simon and collaborators (*19*). It has the broadest range of detections (10^{-7}-10^{-2} M Ca^{2+}), and it is linearly related to pCa, except below 5×10^{-7} M Ca^{2+}. Recently a new ligand has been reported by Simon's group that is linear down to 10^{-8} M. The main disadvantages of the Ca^{2+} microelectrodes are the extremely small area of detection around the tip of the electrode, their very slow response time that is measured in minutes, and the possibility of Ca^{2+} leaks by cell membrane damage. They are best suited to measure slow calcium changes in epithelial layers or tubules in conjunction with microelectrode measurements of membrane potential, Na^+, K^+, and pH in neighboring cells.

By itself, the measurement of $[Ca^{2+}]_i$ can bring much information: the resting levels of calcium, whether or not a stimulus increases or decreases $[Ca^{2+}]_i$, the magnitude of the change, and the sensitivity of the cell to the stimulus. For instance, Figure 11 shows a series of experiments performed by Studer on the effects of epinephrine on isolated rat hepatocytes loaded with aequorin (*20*): *a*) the resting level of Ca_i is around 150 nM; *b*) epinephrine increases $[Ca^{2+}]_i$ in two phases, a peak and a shoulder; *c*) the cells respond to concentrations of epinephrine as low as 5 to 10^{-9} M; and *d*) males are much more responsive than females.

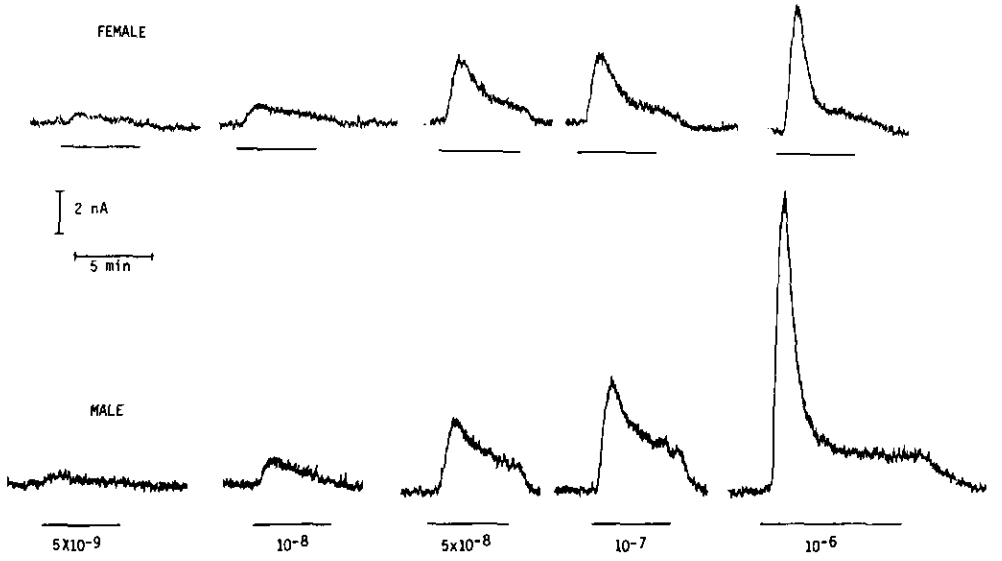

FIGURE 11. *Changes in cytosolic free calcium ($[Ca^{2+}]_i$) as measured by aequorin luminescence ($[Ca^{2+}]_i$) from aequorin-loaded hepatocytes* isolated from male and female rats and perfused with increasing concentrations of epinephrine (from 5×10^{-9} M-10^{-6} M). Packed volume of cells, 0.3 to 0.5 mL were loaded with aequorin by centrifugation, imbedded in agarose gel threads in a cuvette, and perfused at 1 mL/min with Krebs Henseleit buffer at 37°C in an aequorin photometer (*14*). Reprinted with permission from the *American Journal of Physiology.*

To determine whether the rise in cytosolic calcium results from a mobilization of calcium from intracellular organelles or from the extracellular milieu, these experiments can be performed in Ca-free media containing EGTA. Figure 12 shows that the peak $[Ca^{2+}]_i$ evoked by epinephrine is not suppressed in 0 Ca_o^{2+}, but the shoulder disappears until Ca^{2+} is reintroduced in the perfusate, indicating that the peak results from intracellular calcium release while the shoulder is caused by an increased calcium influx.

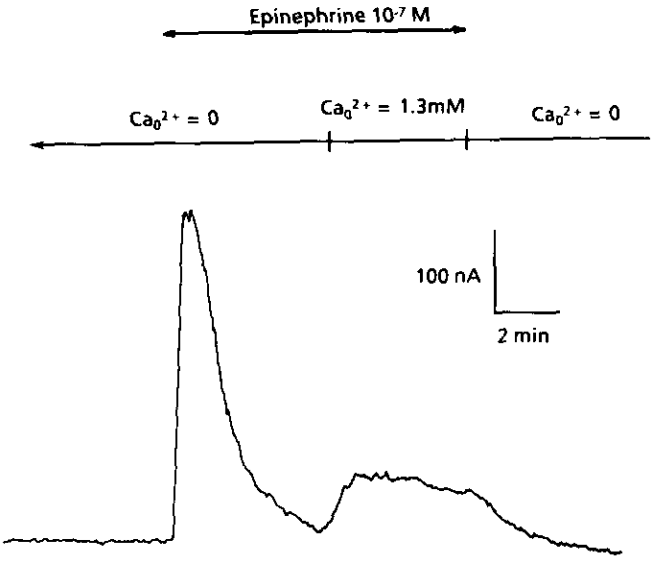

FIGURE 12. Effect of 10^{-7} epinephrine on the cytosolic free calcium of hepatocytes perfused in Ca-free media and measured by aequorin luminescence. The changes in the calcium concentration of the perfusate is indicated above the recording. From Borle (unpublished).

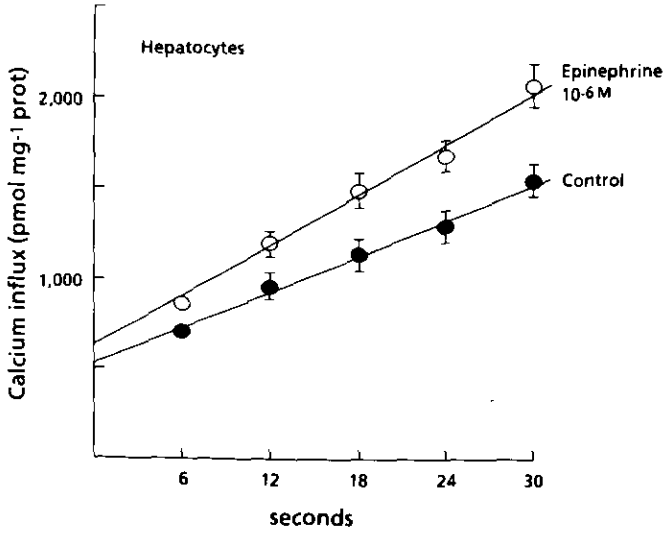

FIGURE 13. Effect of 10^{-6} M epinephrine on calcium influx in isolated rat hepatocytes, measured by zero-time kinetics. From Studer (unpublished).

And indeed, Studer has shown that calcium influx measured by zero-time kinetics is increased by epinephrine (Fig. 13) (R. K. Studer, unpublished).

It is useful to use several methods to focus on a specific problem from different experimental angles. For instance, the rise in $[Ca^{2+}]_i$ observed after anoxia (*21*) or after lowering the extracellular Na^+ by substitution with TMA (*22*) (Fig. 14) does not take place in the absence of extracellular Ca^{2+} eliminating the contribution of intracellular calcium sources (*21,22*). The rise in $[Ca^{2+}]_i$ could be caused by a decreased calcium efflux on the Na^+-Ca^{2+} antiporter operating either in the forward mode (Ca^{2+}_i vs. Na^+_o) or by an increased calcium influx on the antiporter operating in the reverse mode (Ca^{2+}_o vs. Na^+_i). Figure 15 shows that Na^+_o substitution by TMA stimulates calcium efflux proving that the rise in $[Ca^{2+}]_i$ is not caused by a decreased Ca efflux. On the other hand, Na^+ substitution with TMA stimulates Ca^{2+} influx when measured by zero-time kinetics (Fig. 16). The sum of these three experimental approaches suggests that lowering extracellular Na^+ stimulates the reverse mode of the Na^+-Ca^{2+} antiporter by increasing the calcium influx in exchange for an increased Na^+ efflux which we have also documented experimentally (*22*).

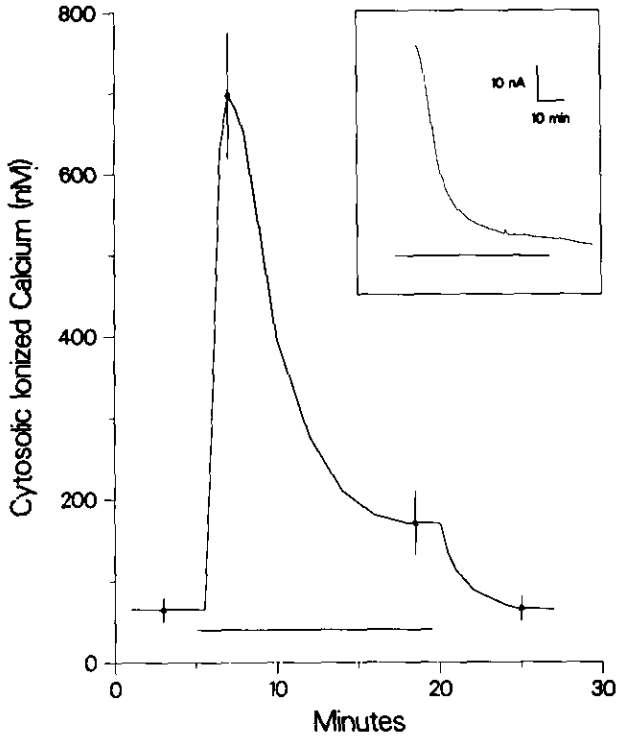

FIGURE 14. Composite drawing from five recordings showing the effects of the total replacement of extracellular Na^+ with 120 mM TMA chloride and 24 mM choline bicarbonate on the cytosolic-ionized calcium measured with aequorin in monkey kidney cells. The period of Na^+-free perfusion is indicated by the horizontal line below the tracing. Inset: original recording of one typical experiment (*22*); reprinted with permission from the *Journal of Biological Chemistry*.

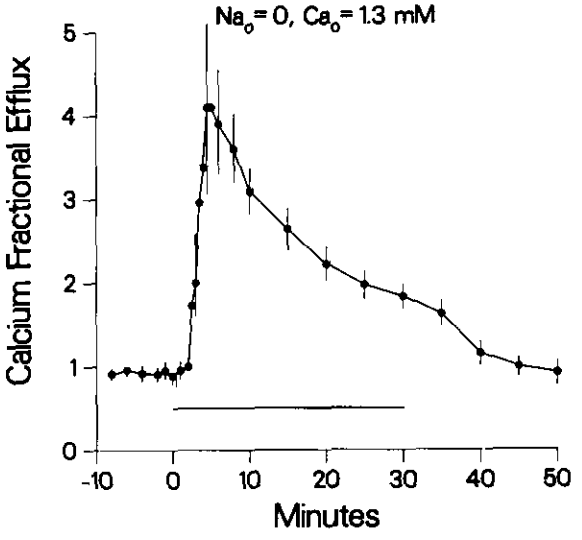

FIGURE 15. Effect of the total removal of extracellular Na^+ on calcium efflux from monkey kidney cells. Calcium fractional efflux measured with ^{45}Ca represents the experimental to control ratio. Effect of perfusion with a medium in which Na^+ was replaced by 120 mM TMA and 24 mM choline bicarbonate in the presence of 1.3 mM Ca^{2+}. The period of Na^+-free perfusion is indicated by the horizontal line below the graph. Each data point represents the mean ± SE of four experiments (*22*); reprinted with permission from the *Journal of Biochemical Chemistry*.

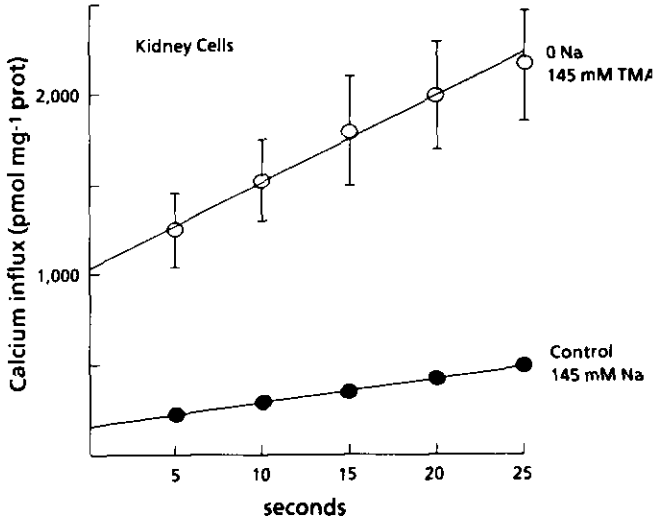

FIGURE 16. Effect of the total replacement of extracellular Na^+ on calcium influx in kidney cells measured by ^{45}Ca zero-time kinetics. The measurement of the experimental group (addition of ^{45}Ca) was started 30 sec after the cells were exposed to the Na-free medium. From Borle (unpublished).

More information can be obtained by quantitatively comparing the rise in $[Ca^{2+}]_i$, evoked by a stimulus and the consequent rise in calcium efflux from the cells. For instance, in my laboratory, Freudenrich showed that adrenalectomy in male rats increases the resting $[Ca^{2+}]_i$, but dampens the rise in $[Ca^{2+}]_i$ evoked by epinephrine (*23*) (Fig. 17). As a consequence, the rise in Ca^{2+} efflux is also depressed by adrenalectomy (Fig. 18). However, when one compares the rise in Ca efflux for a given rise in $[Ca^{2+}]_i$ (Fig. 19), it appears that for the same increase in $[Ca^{2+}]_i$, calcium efflux is significantly less in adrenalectomy. This suggests a deficiency in the active calcium transport system, presumably a depressed calcium pump activity.

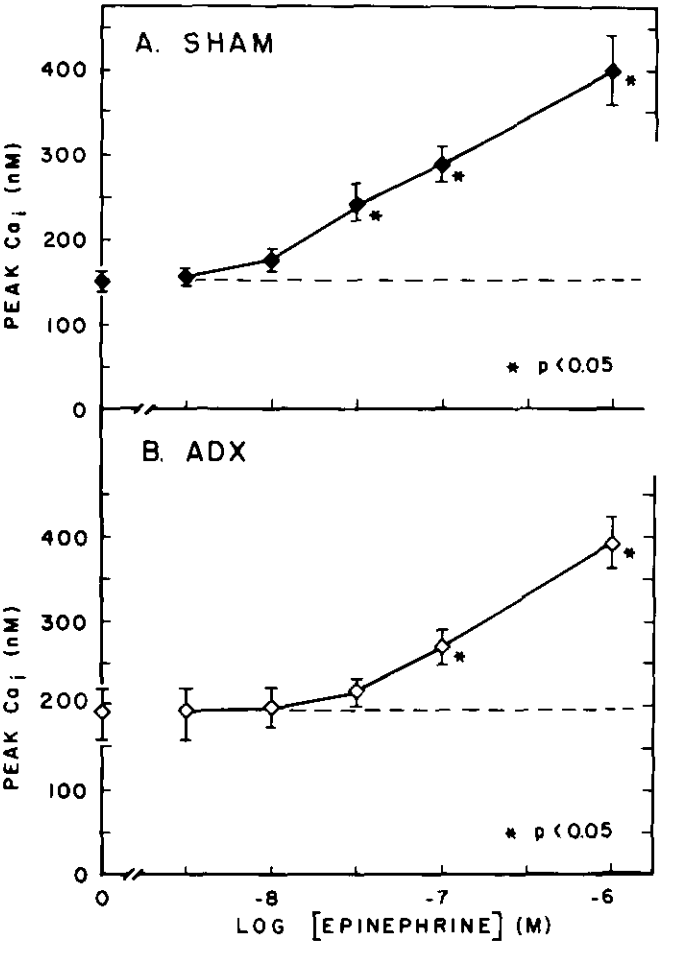

FIGURE 17. Resting and epinephrine-stimulated concentration of cytosolic free calcium in hepatocytes from sham (*A*) and adrenalectomized (*B*) rats measured with aequorin. Data represents mean ± SE of eight sham and eight adx experiments. Significant difference ($p < 0.05$) above the resting level (dotted line) are denoted by an asterisk (*) (*23*); reprinted with permission from the *Journal of Biological Chemistry*.

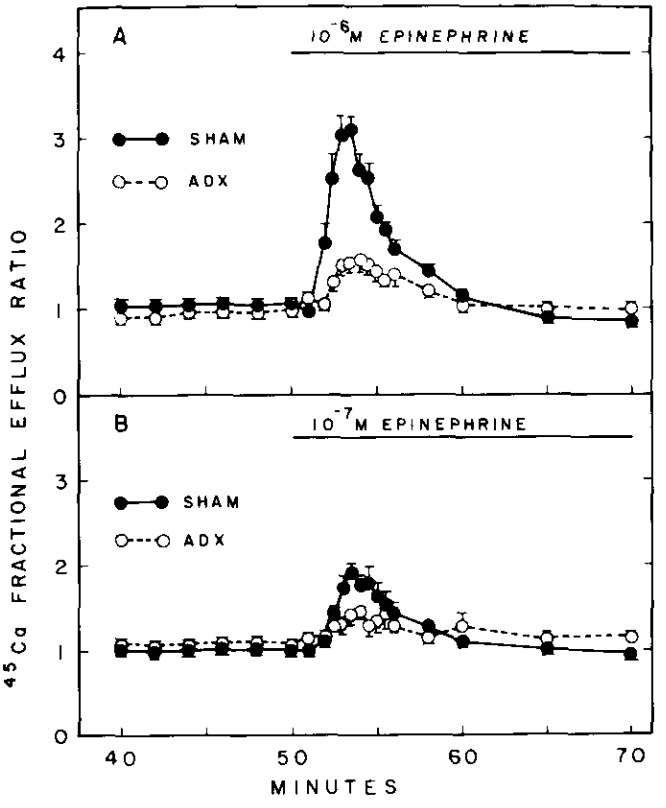

FIGURE 18. Increases in calcium efflux in response to 10^{-6} M (graph *A*) and 10^{-7} M (graph *B*) epinephrine in hepatocytes from sham (●) and adrenalectomized (○) rats. Fractional efflux ratio is the ratio of the efflux from stimulated cells to that from unstimulated cells perfused concurrently. Each data point represents the mean ± SE of eight experiments in each group. From Freudenrich and Borle (*23*); reprinted with permission from the *Journal of Biological Chemistry*.

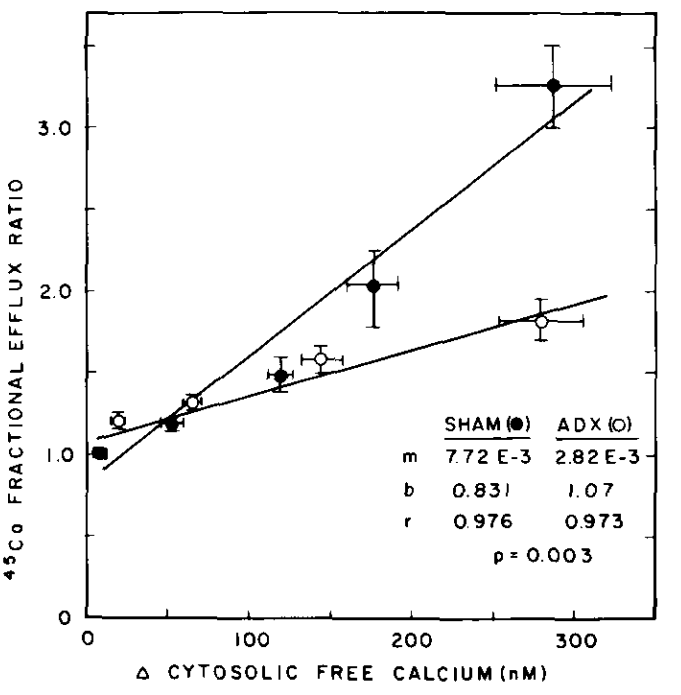

FIGURE 19. Relationship between calcium efflux and the change in cytosolic free calcium measured with aequorin ($\Delta[Ca^{2+}]_i$) in response to epinephrine in hepatocytes from sham and adrenalectomized rats. The peak fractional calcium efflux is plotted as a function of $\Delta [Ca^{2+}]_i$ at various epinephrine concentration. The two measurements were made in the same cell preparations. Each point represent the mean ± SE of eight experiments in each group. The regression lines were determined by least squares and analyzed for significant difference ($p < 0.05$) by analysis of covariance. The slope (m), *y*-intercept (b), and correlation coefficient (*r*) of each regression line are shown in the figure. From Freudenrich and Borle (*23*); reprinted with permission from the *Journal of Biological Chemistry*.

Isolated Organelles and Vesicles

It is also possible to study the kinetic properties of specific organelles or specific calcium transport mechanisms such as (Ca^{2+}-Mg^{2+}) ATPase-dependent calcium transport, Na^+-Ca^{2+} antiporters, and Ca^{2+} channels in broken cell systems. These transporters have been isolated within plasma membrane vesicles or incorporated into artificial membranes or liposomes. The calcium transport properties of isolated mitochondria or endoplasmic reticulum have been under study for many years. Recently, patch clamps and whole cell patches have been used to study single calcium channels and intracellular signaling systems. I shall only mention these techniques since I have no expertise in any of them. In these model systems, the advantage of controlling the experimental conditions are offset by the possibility that these are not physiological conditions. Thus, the information obtained from these isolated systems may not always reflect their behavior in an intact cell and their relative role and importance in the control of cell calcium metabolism.

Calciotropic Drugs

Finally, a few words of caution should be offered regarding the various drugs or chemicals used as Ca^{2+} ionophores, Ca^{2+} blockers, and as agonists or antagonists of calcium transport processes. Few if any of these agents are specific, but they are often thought to be so, and their expected effects are sometimes assumed to occur without independent verification. For instance, A23187 is not only a calcium ionophore but also a proton ionophore. It increases $[Ca^{2+}]_i$, but it does not necessarily increase net calcium influx into cells, since most cells lose 50 to 70% of their calcium after the administration of A23187 (*24*).

Verapamil is a calcium channel blocker, but it also inhibits Na^+-Ca^{2+} exchange, and it is a powerful α-adrenergic blocker (*25*). Nifedipine and diltiazem are both calcium channel blockers, but both increase $[Ca^{2+}]_i$ in kidney cells and in hepatocytes at concentrations of 10^{-9} M and 10^{-3} M, respectively (Borle, unpublished). Amiloride, dichlorobenzamil, and dimethylbenzamil are used as blockers of the Na^+-Ca^{2+} and Na^+-H^+ antiporters, but all three increase

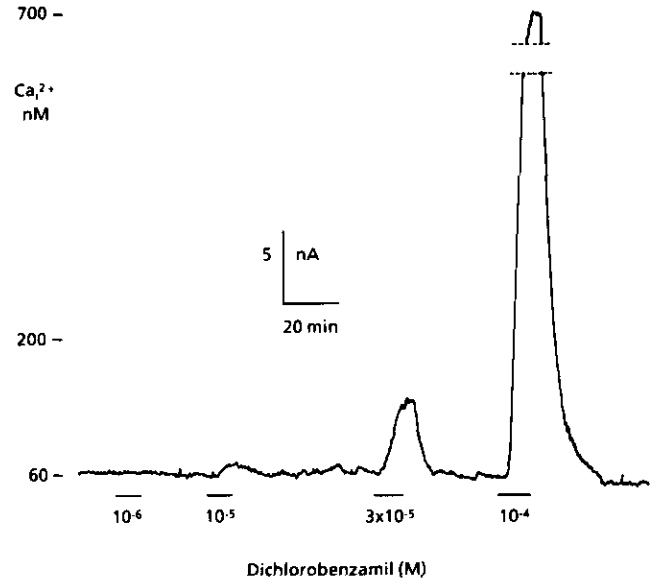

FIGURE 20. Effect on increasing concentration of dichlorobenzamil on the cytosolic free calcium of kidney cells (MDCK) measured with aequorin. From Borle (unpublished).

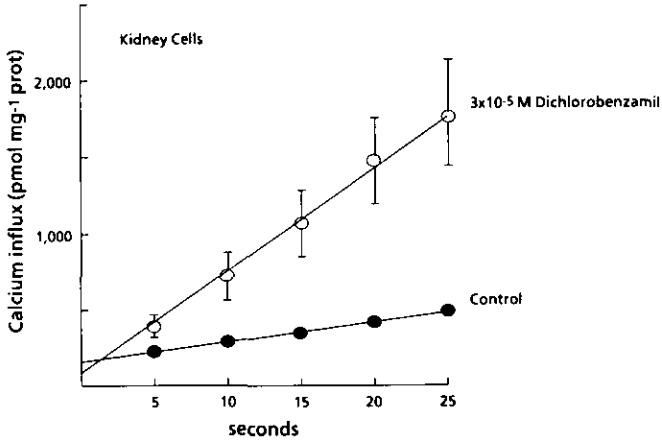

FIGURE 21. Effect of 2×10^{-5} M dichlorobenzamil on calcium influx in kidney cells (MDCK) measured by zero-time kinetics of ^{45}Ca uptake. From Borle (unpublished).

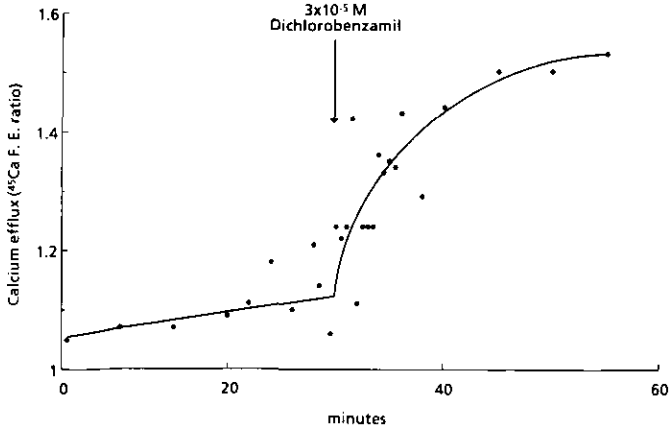

FIGURE 22. Effect of 2×10^{-5} M dichlorobenzamil on calcium efflux in kidney cells. From Borle (unpublished).

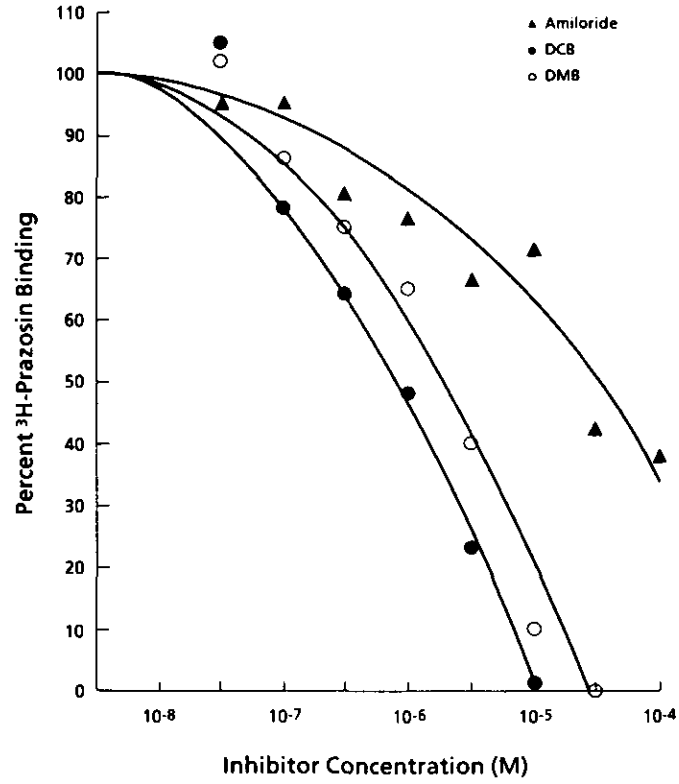

FIGURE 23. Effect of amiloride, dichlorobenzamil, and dimethylbenzamil on prazocin binding to intact hepatocytes isolated from rats. From Studer and Borle (unpublished).

$[Ca^{2+}]_i$ in kidney and liver cells at concentrations as low or lower than their K_I (Fig. 20). Dichlorobenzamil also dramatically increase calcium influx in kidney cells (Fig. 21), and because of the high cytosolic calcium, it enhances calcium efflux (Fig. 22). Amiloride, dichlorobenzamil, and dimethylbenzamil are also powerful α-adrenergic antagonists (Fig. 23). The effects of calciotropic drugs on several parameters of cell calcium metabolism should be carefully surveyed before their assumed specific mode of action can be accepted.

Conclusion

In conclusion, many methods are available to study cell calcium metabolism, $[Ca^{2+}]_i$, calcium distribution, and calcium fluxes. Beyond recognizing the assets and drawbacks of each technique, the safest approach to study a particular problem involving cell calcium is to use several different methods, focusing on it from different angles.

This work was supported by the following grants: National Science Foundation PCM 8305, NIH DK 35320, and National Diary Council. We acknowledge the collaboration of T. Uchikawa, R. K. Studer, K. W. Snowdowne, and C. C. Freudenrich in some aspects of methods development.

REFERENCES

1. Borle, A. B. Control, modulation and regulation of cell calcium. Rev. Physiol. Biochem. Pharmacol. 90: 13–153 (1981).
2. Reinhart, P. H., Taylor, W. M., and Bygrave, F. L. A procedure for the rapid preparation of mitochondria from rat liver. Biochem. J. 204: 731–735 (1984).
3. Weibel, E. R., Staubli, W., Gnagi, H. R., and Hess, F. A. Correlated morphometric and biochemical studies on the liver cell, I. Morphometric model, stereologic methods and normal morphometric data for rat liver. J. Cell. Biol. 42: 68–91 (1969).
4. Bond, M., Vadasz, G., Somlyo, A. V., and Somlyo, A. P. Subcellular calcium and magnesium mobilization in rat liver stimulated *in vivo* with vasopressin and glucagon. J. Biol. Chem. 262: 15630–15636 (1987).
5. Uchikawa, T., and Borle, A. B. Studies of calcium-45 desaturation from kidney slices in flow-through chambers. Am. J. Physiol. 234: R34–R38 (1978).
6. Uchikawa, T., and Borle, A. B. Solutions for the kinetic analysis of ^{45}calcium uptake curves. Cell Calcium 2: 173–186 (1981).
7. Borle, A. B. Pitfalls of the ^{45}Ca uptake method. Cell Calcium 2: 187–196 (1981).
8. Shepard, C. W. Basic Principles of the Tracer Method. John Wiley and Sons, New York, 1962.
9. Jacquez, J. A. Compartmental Analysis in Biology and Medicine. Elsevier Biomedical Press, New York, 1972.
10. Borle, A. B., Uchikawa, T., and Anderson, J. H. Computer simulation and interpretation of ^{45}Ca efflux profile patterns. J. Membrane. Biol. 68:37–46 (1982).
11. Blinks, J. R., Wier, G. W., Hess. P., and Pendergast, F. G. Measurement of Ca^{2+} concentration in living cells. Prog. Biophys. Mol. Biol. 40: 1–114 (1982).
12. Tsien, R. Y., and Rink, T. J. Measurement of free Ca^{2+} in cytoplasm. In: Current Methods in Cellular Neurobiology (J. L. Baker and Y. F. McKelvy, Eds.), John Wiley and Sons, New York, 1983, pp. 249–312.
13. Borle, A. B., and Snowdowne, K. W. Methods for the measurement of intracellular ionized calcium in mammalian cells: comparison of four classes of Ca^{2+} indicators. In: Calcium and Cell Function, Vol. 7 (W. Y. Cheung, Ed.), Academic Press, New York, 1987, pp. 159–200.
14. Borle, A. B., and Snowdowne, K. W. Measurement of intracellular ionized calcium with aequorin. Methods Enzymol. 124: 90–116 (1986).
15. Borle, A. B., Freudenrich, C. C., and Snowdowne, K. W. A simple method for incorporating aequorin into mammalian cells. Am. J. Physiol. 251: C323–C326 (1986).
16. Tsien, R. Y., Pozzan, T., and Rink, T. J. Calcium homeostasis in intact lymphocytes: cytoplasmic free calcium monitored with a new intracellular trapped fluorescence indicator. J. Cell. Biol. 94: 325–334 (1982).
17. Grynkiewicz, G., Poenie, M., and Tsien, R. Y. A new generation of Ca^{2+} indicators with greatly improved fluorescent properties. J. Biol. Chem. 260: 3440–3450 (1985).
18. Scarpa, A., Brinley, F. J., Tiffert, T., and Dubyak, G. R. Metallochromic indicators of ionized calcium. Ann. N. Y. Acad. Sci. 307: 86–111 (1978).
19. Oehme, M., Kessler, M., and Simon, W. Neutral carrier Ca^{2+}-microelectrode. Chimia 30: 204–206 (1976).
20. Studer, R. K. Sexual dimorphism in adrenergic regulation of heptic glycogenolysis. Am. J. Physiol. 252: E467–E476 (1987).
21. Snowdowne, K. W., Freudenrich, C. C., and Borle, A. B. The effects of anoxia on cytosolic free calcium, calcium fluxes and cellular ATP level in cultured kidney cells. J. Biol. Chem. 260: 11619–11626 (1985).
22. Snowdowne, K. W., and Borle, A. B. Effects of low extracellular sodium on cytosolic iodized calcium. Na^{+}-Ca^{2+} exchange as a major calcium pathway in kidney cells. J. Biol Chem. 260: 14998–15007 (1985).
23. Freudenrich, C. C., and Borle, A. B. The effects of adrenalectomy on the α-adrenergic regulation of cytosolic free calcium in hepatocytes. J. Biol. Chem., in press.
24. Borle, A. B., and Studer, R. K. Effects of ionophores on the transport and distribution of calcium in isolated cells and in liver and kidney slices. J. Membrane Biol. 38: 51–72 (1978).
25. Blackmore, P. F., El Refai, M. F., and Exton, T. H. α-adrenergic blockade and A23187 mediated Ca^{2+} uptake by the calcium antagonist verapamil in rat liver cells. Molec. Pharmacol. 15: 598–606 (1979).
26. Studer, R. K., and Borle, A. B. Effect of pH on the calcium metabolism of isolated rat kidney cells. J. Membrane. Biol. 48: 325–341 (1979).
27. Borle, A. B., and Clark, I. Effect of phosphate induced hyperparathyroidism and parathyroidectomy on rat kidney calcium *in vivo*. Am. J. Physiol. 241: E1356–E141 (1981).
28. Studer, R. K., and Borle, A. B. Sex difference in cellular calcium metabolism of rat hepatocytes and in α-adrenergic activation of glycogen phosphorylase. Biochem. Biophys. Acta 762: 302–314 (1988).
29. Studer, R., and Borle, A. B. Effect of adrenalectomy on cellular calcium metabolism and on the response to adrenergic stimulation of hepatocytes isolated from male and female rats. Biochem. Biophys. Acta 804: 377–385 (1984).
30. Studer, R. K. Changes in basal and stimulated hepatocyte calcium metabolism in diabetes. Endocrinology, submitted.